

Supplementary Information

One-pot synthesis of robust dendritic sulfur quantum dots for two-photon fluorescence imaging and “off-on” detection of hydroxyl radical and ascorbic acid

Jisuan Tan^a, Yiheng Song^a, Xuanjun Dai^a, Guan Wang^b, Li Zhou^{a,*}

^a *Key laboratory of New Processing Technology for Nonferrous Metal and Materials (Ministry of Education), Guangxi Key Laboratory of Optical and Electronic Materials and Devices, and College of Materials Science and Engineering, Guilin University of Technology, Guilin 541004, China*

^b *Institute of Sustainability for Chemicals, Energy and Environment, A*STAR, Singapore, 138634, Singapore*

*Corresponding author.

E-mail address: zhouli@glut.edu.cn (L. Zhou)

1. Materials

Sublimed sulfur (99.95%), ascorbic acid (AA, 99%), sodium hydroxide (NaOH), hydrogen peroxide (H₂O₂, 35 wt%), histidine, glycine, arginine, cysteine, glucose, lysine, glutathione, thiazolyl blue tetrazolium bromide (MTT, 98%), and various metal salts were purchased from Innochem Co., Ltd. (Beijing, China) and used as received. High purity oxygen (O₂, 99.999%) was purchased from Huaao Gas Co., Ltd. (Liuzhou, China). All used water was ultrapure water (18.2 MΩ). Hyperbranched polyglycerol (HPG, $M_n = 3100$ Da, PDI = 1.48) was synthesized by anionic ring-opening polymerization of glycidol according to our previous report.¹

2. Characterization

Fourier Transform Infrared Spectroscopy (FTIR) measurement was conducted on a Thermo Nexus 470 FT-IR instrument using KBr tablet method in the range of 4000-400 cm⁻¹. Raman spectra were recorded on a LabRam-1B Raman spectroscope with 532.05 nm incident radiation and a 50 × aperture. Transmission electron microscopy (TEM) observation was carried out on a JEOL-2010 TEM with 150 kV accelerating voltage. X-ray photoelectron spectroscopy (XPS) measurements were conducted on Kratos AXIS UltraDLD (Kratos Analytical Ltd.) with mono Al K α radiation ($h\nu=1487.71$ eV) at a power of 75 W. UV/vis absorption spectra were determined by a Shimadzu UV-3600 UV-VIS-NIR spectrophotometer. The photoluminescence spectra were collected at room temperature using a Varian Cary 100 fluorescence spectrophotometer. The absolute photoluminescence quantum yield (QY) of HPG-SQDs solution was determined on a FluoroMax-4 (HORIBA) photoluminescence spectrometer equipped with an integrating sphere, and the excitation wavelength is 330 nm. Confocal laser-scanning microscopy (CLSM, Olympus FV3000) images were collected with excitation wavelength at 405 nm. Two-photon fluorescence spectra and images were obtained by a multiphoton fluorescence microscope (TCS SP8 DIVE, Leica, Germany). Elemental analysis (EA) measurement was performed on a Perkin-Elmer 240C Elemental Analytical Instrument. The standard deviation (σ) was calculated according to the following equation:

$$\sigma = \sqrt{\frac{\sum_{i=1}^N (S_i - S_{av})^2}{N}} \quad (1)$$

where N represents the number of samples, S_i means a single sample value, and S_{av} is the average value of all samples.

3. Preparation of hyperbranched polyglycerol-capped sulfur quantum dots (HPG-SQDs)

Fluorescent HPG-SQDs can be easily synthesized by one-pot reaction under pure oxygen atmosphere. In a typical procedure, sublimed sulfur (1.6 g), HPG (1.0 g) and NaOH (4.0 g) were added to 50 mL of deionized water in a 100 mL flask. The mixture was stirred at 95 °C in a pure oxygen atmosphere. After stirring for 24 h, the resulting mixture was dialyzed against water with a dialysis bag (molecular weight cutoff = 5000 Da), and then freeze-dried to afford purified HPG-SQDs.

4. Sensing of hydroxyl radical (\bullet OH)

The \bullet OH was formed by Fenton reaction between H_2O_2 and Fe^{2+} . For sensing of \bullet OH, typically, 980 μ L of aqueous solution of HPG-SQDs (50 μ g/mL) and 20 μ L of \bullet OH with different concentrations (0–1.2 mM) were mixed in a cuvette by shaking at room temperature for 2 min. Fluorescent spectra of the mixture were determined on a Varian Cary 100 fluorescence spectrophotometer at 25 °C with excitation at 330 nm and 420 nm, respectively. Correspondingly, the fluorescence intensity at the wavelength of 434 nm and 501 nm were recorded.

5. Sensing of ascorbic acid (AA)

For detection of AA, the mixture of HPG-SQDs and \bullet OH was employed as a sensing system. In a typical procedure, 900 μ L of the mixture of HPG-SQDs (50 μ g/mL) and \bullet OH (24 μ M) was added to a quartz cuvette. Subsequently, 100 μ L of AA solution with known concentration (0–16 mM) was added to the mixture of HPG-SQDs/ \bullet OH. After shaking the mixture for 3 min, the emission spectra of mixture were collected with excitation at 330 nm and 420 nm, respectively.

6. Cytotoxicity evaluation

The cytotoxicity of HPG-SQDs and PEG-SQDs was assessed using the standard MTT assay. Firstly, HeLa cervical cancer cells were seeded in 96-well plates at a

density of 1×10^4 cells/mL. After 24 h of incubation, the culture medium was replaced by the aqueous solution of HPG-SQDs (or PEG-SQDs) with concentrations of 200, 100, 50, 25, and 0 $\mu\text{g/mL}$ and further incubated for 24 h. Subsequently, the wells were washed thrice with PBS buffer, and 100 μL of freshly prepared MTT (0.5 mg/mL) solution in culture medium was added to each well. The MTT medium solution was carefully removed after 3 h of incubation. Dimethyl sulfoxide (100 μL) was then added into each well, and the plate was gently shaken for 20 min. The absorbance of MTT at 570 nm was recorded by the microplate reader. Cell viability was expressed by the ratio of absorbance of the cells incubated with HPG-SQDs (or PEG-SQDs) to that of the cells incubated with culture medium only.

7. Single-photon fluorescence imaging

Typically, HeLa cells were cultured in Dulbecco's modified Eagle's medium at 37 $^{\circ}\text{C}$ for 12 h under 5% CO_2 . After removing the growth medium, medium containing HPG-SQDs (50 $\mu\text{g/mL}$) was added to incubate with the HeLa cells for 2 h at 37 $^{\circ}\text{C}$. Subsequently, the cells were rinsed with phosphate buffer to remove free HPG-SQDs. After washing with PBS buffer for two times, imaging of HeLa cells was conducted on a confocal laser-scanning microscopy (CLSM, Olympus FV3000).

8. Two-photon fluorescence imaging

HeLa cells in chamber were cultured at 37 $^{\circ}\text{C}$ for 24 h. When the cells density reaches 80% of the culture plate, the cells were incubated with culture medium and HPG-SQDs (50 $\mu\text{g/mL}$) for 2 h. After that, the cells were washed twice with phosphate buffer to remove the unbound HPG-SQDs. In order to monitor $\bullet\text{OH}$ and AA in cells, the HPG-SQDs-stained HeLa cells were further treated with $\bullet\text{OH}$ (30 μM) and AA (1.5 mM). Subsequently, the two-photon fluorescence images of cells were recorded by TCS SP8 DIVE multiphoton fluorescence microscope (Leica, Germany) with femtosecond laser pulse.

Table S1. Elemental analysis result of HPG-SQDs.

Element	Content (wt %)
S	32.48
C	30.37
H	6.23
O	30.92 (Calculated)

Table S2. Comparison of different fluorescent nanoprobe for sensing of •OH.

Detection	Fluorescent nanoprobe	Linear range (μM)	Limit of detection (μM)	Reference
•OH	Coumarin-activated silica nano hybrid	0.5-200	1.65	[2]
•OH	Silicon quantum dots	1-200	0.97	[3]
•OH	Mn-doped silicon quantum dots	0.8-50	0.88	[4]
•OH	Boron-doped carbon quantum dots	1.2-500	0.37	[5]
•OH	Terephthalic acid tailored graphene quantum dots	0.018-6	0.12	[6]
•OH	HPG-SQDs	0.5-20	0.23 ± 0.03	This work

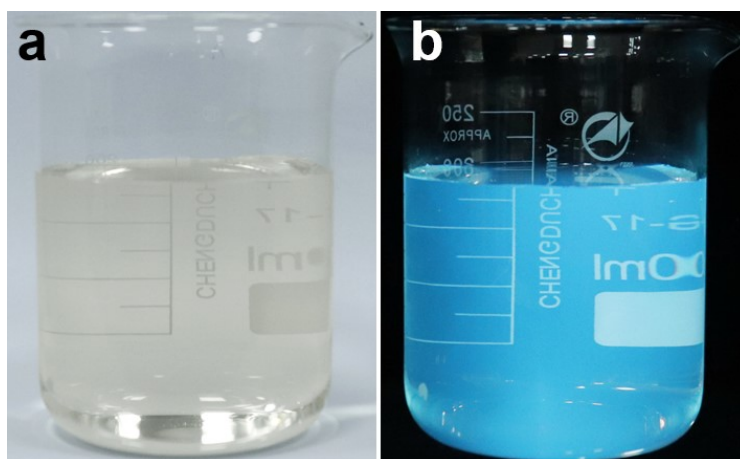


Fig. S1. Photographs of aqueous solution of HPG-SQDs under daylight (a) and under 365 nm UV lamp (b).

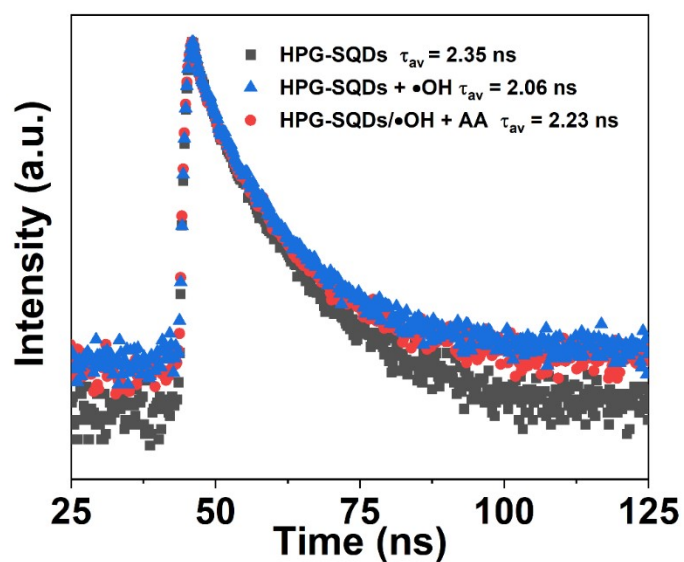


Fig. S2. Fluorescence-decay curves of HPG-SQDs before and after mixing •OH (20 μ M) and AA (1.6 mM).

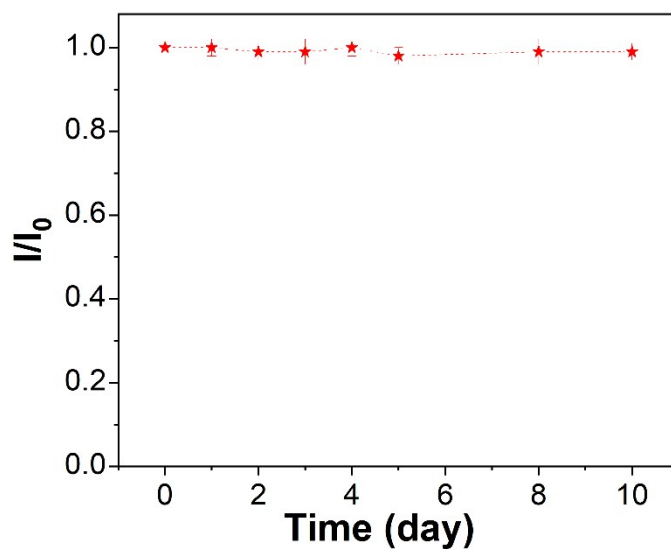


Fig. S3. Effect of storage time on the fluorescence intensity of HPG-SQDs ($\lambda_{\text{ex}} = 330$ nm). I_0 represents the fluorescence intensity of prepared HPG-SQDs solution. I represents the fluorescence intensity of HPG-SQDs solution after storage for different days.

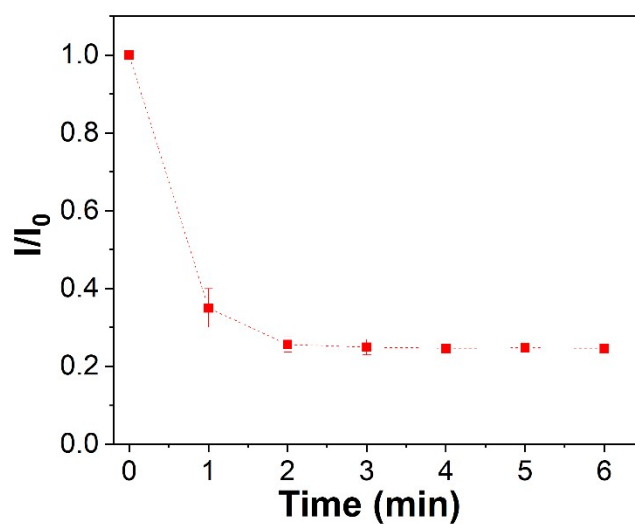


Fig. S4. I/I_0 value of HPG-SQDs against time after mixing $20 \mu\text{M}$ of $\bullet\text{OH}$ ($\lambda_{\text{ex}} = 330$ nm). I_0 and I represent the fluorescence intensity of HPG-SQDs in the absence and presence of $20 \mu\text{M}$ of $\bullet\text{OH}$, respectively.

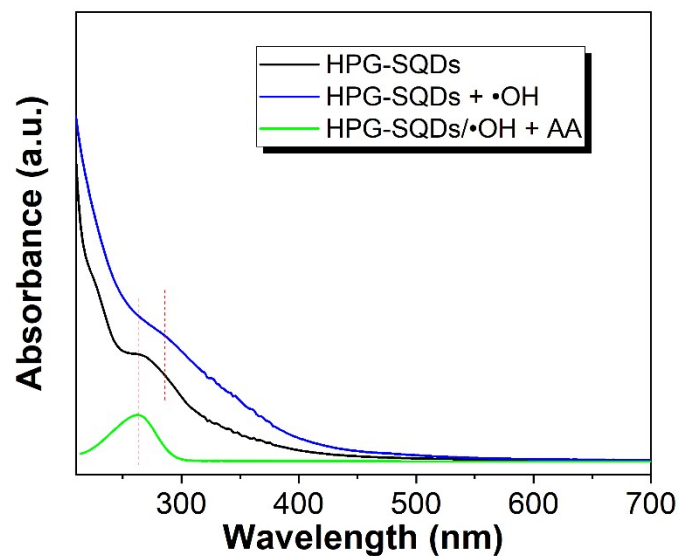


Fig. S5. UV/vis absorption spectra of HPG-SQDs, the mixture of HPG-SQDs and •OH before and after mixing with AA.

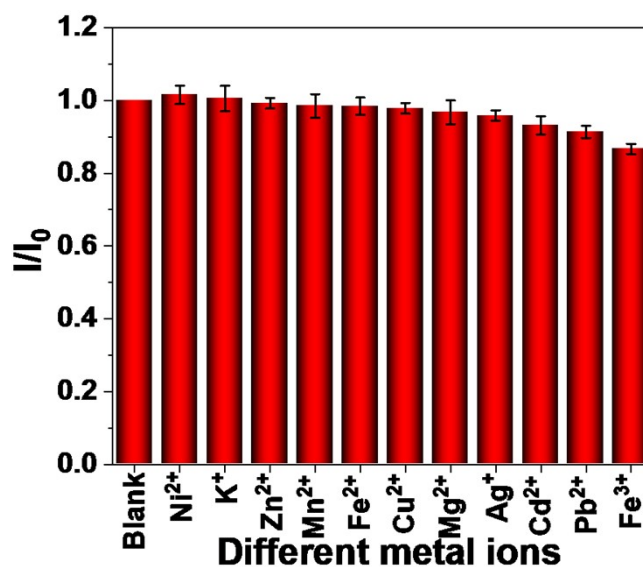


Fig. S6. Effect of mixing 50 μ M different metal ions on I/I_0 value of HPG-SQDs. I and I_0 represent the fluorescence intensity of HPG-SQDs in the presence and absence of metal ions, respectively ($\lambda_{\text{ex}} = 330$ nm).

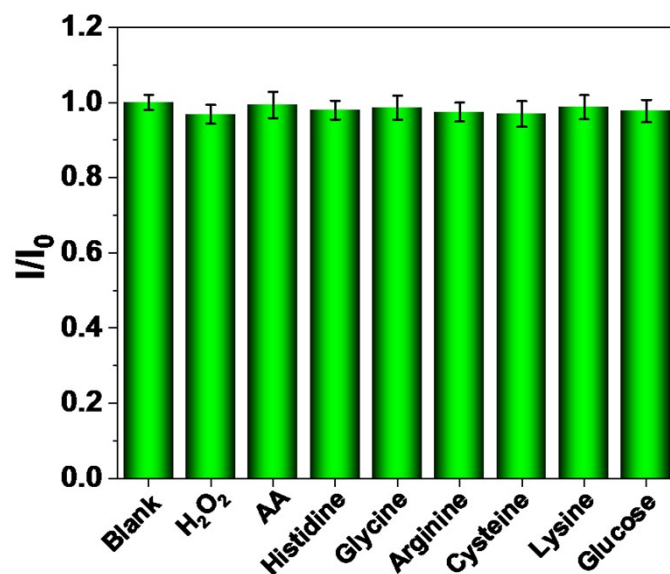


Fig. S7. Effect of mixing 50 μM various molecules on I/I_0 value of HPG-SQDs. I and I_0 represent the fluorescence intensity of HPG-SQDs in the presence and absence of various molecules, respectively ($\lambda_{\text{ex}} = 330 \text{ nm}$).

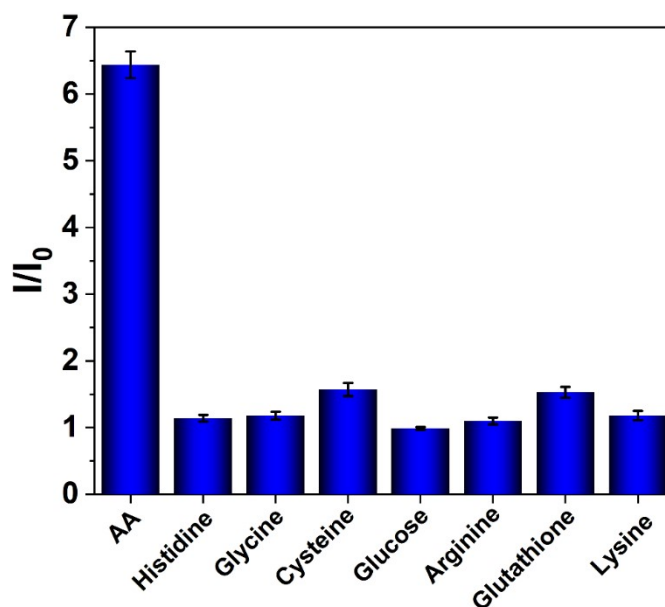


Fig. S8. Effect of mixing 10 mM various molecules on I/I_0 value of HPG-SQDs/ $\bullet\text{OH}$ system. I_0 and I represent the fluorescence intensity of HPG-SQDs/ $\bullet\text{OH}$ system before and after mixing various molecules, respectively ($\lambda_{\text{ex}} = 330 \text{ nm}$).

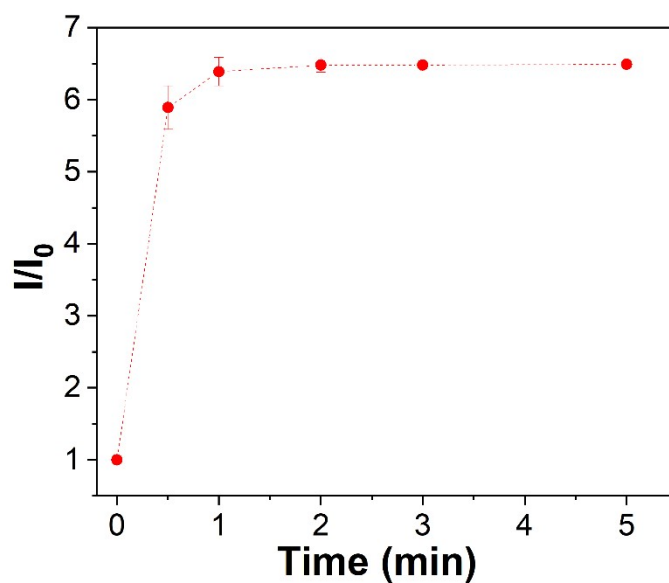


Fig. S9. I/I_0 value of HPG-SQDs/ \bullet OH system against time after mixing 1 mM of AA ($\lambda_{\text{ex}} = 330$ nm). I_0 and I represent the fluorescence intensity of HPG-SQDs/ \bullet OH system in the absence and presence of 1 mM of AA, respectively.

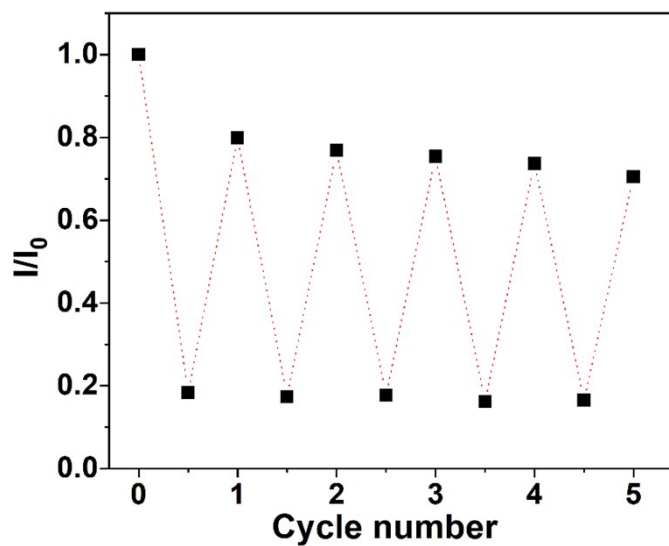


Fig. S10. I/I_0 value of HPG-SQDs after repeated addition of \bullet OH (24 μ M) and AA (1.6 mM) ($\lambda_{\text{ex}} = 330$ nm).

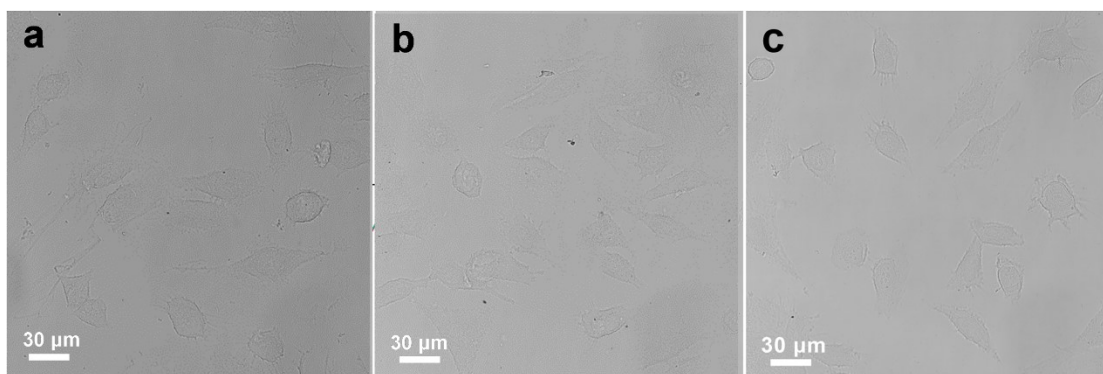


Fig. S11. Two-photon bright field images of HeLa cells after incubation with HPG-SQDs (a) and followed by addition of $\bullet\text{OH}$ (b) and AA (c).

References

- [1] L. Zhou, C. Gao, X. Hu and W. Xu, *Chem. Mater.*, 2011, **23**, 1461–1470.
- [2] S. Liu, J. Zhao, K. Zhang, L. Yang, M. Sun, H. Yu, Y. Yan, Y. Zhang, L. Wu and S. Wang, *Analyst*, 2016, **141**, 2296–2302.
- [3] Q. Zhao, R. Zhang, D. Ye, S. Zhang, H. Chen and J. Kong, *ACS. Appl. Mater. Inter.*, 2017, **9**, 2052–2058.
- [4] Y. Sun, L. Pang, X. Guo and H. Wang, *Microchim. Acta.*, 2022, **189**, 60.
- [5] X. An, Q. Tan, S. Pan, S. Zhen, Y. Hu and X. Hu, *Microchim. Acta.*, 2022, **189**, 148.
- [6] X. Hai, Z. Guo, X. Lin, X. Chen and J. Wang, *ACS. Appl. Mater. Inter.*, 2018, **10**, 5853–5861.